Supplementary Figures

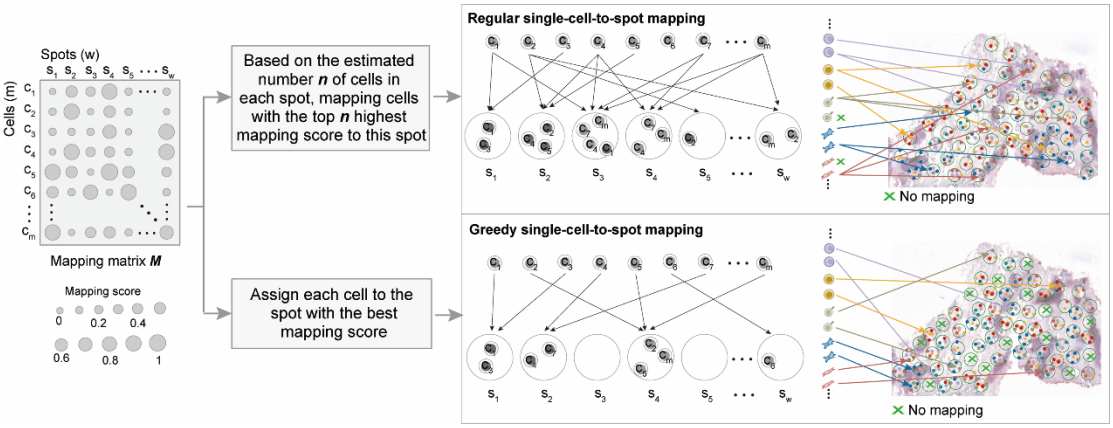

Supplementary Fig. 1. Schema comparing Celloc's regular and greedy single-cell-to-spot mapping tasks. For regular single-cell-to-spot mapping, based on the estimated number *n* of cells in each spot, Celloc mapped cells with the top *n* highest mapping score to this spot. The regular mapping aimed to fill ST spots with suitable number of cells from scRNA-seq to enhance the quality of ST data in terms of resolution and gene expression quantity. For greedy single-cell-to-spot mapping, Celloc assigned each cell to the spot with the best mapping score. The greedy mapping aimed to assign the spatial location for every cell in scRNA-seq data to completely investigate the spatial pattern across the full scRNA-seq dataset.

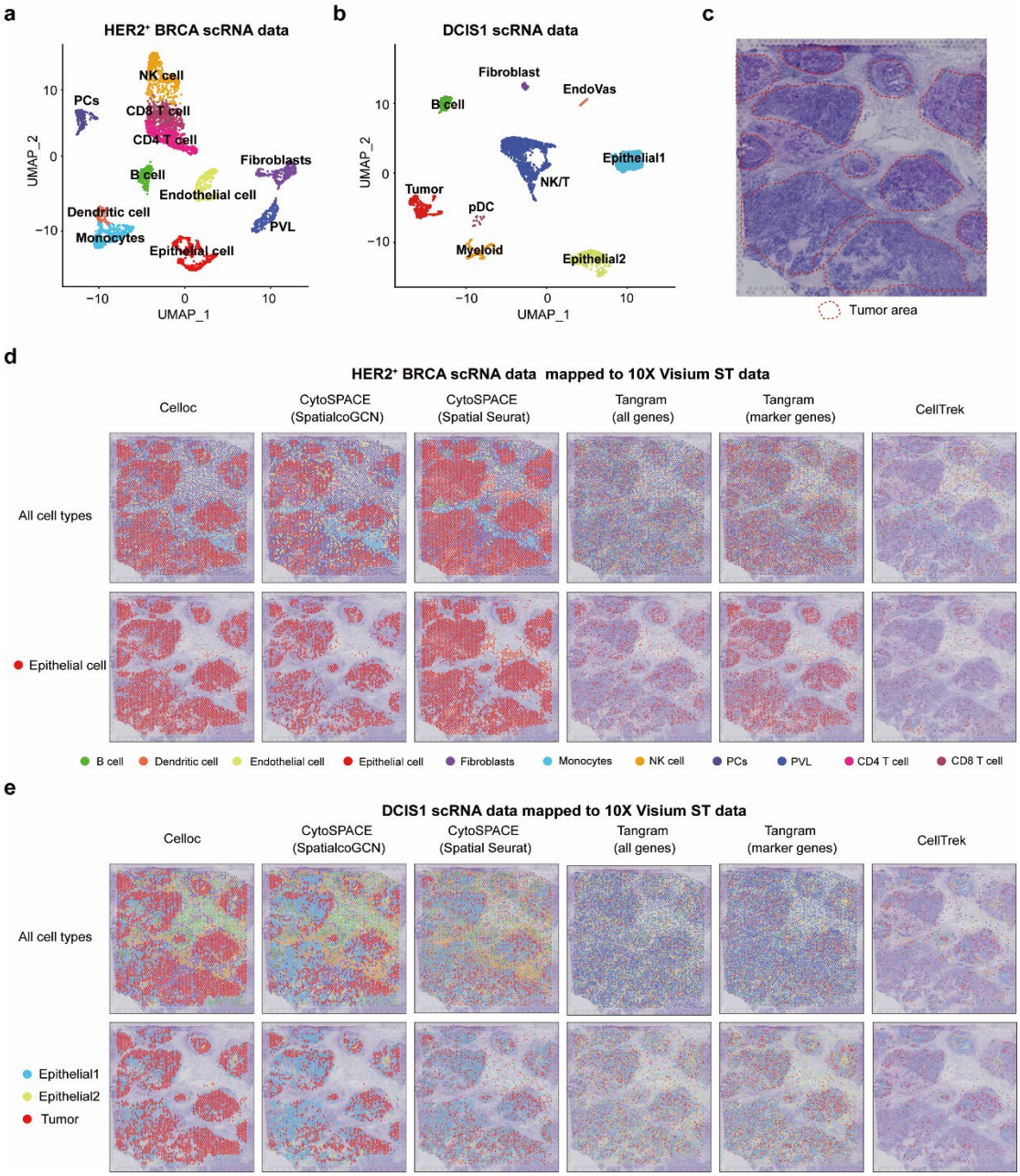

Supplementary Fig. 2. Visualization of (regular) mapping results of breast cancer ST dataset (sample2) with different scRNA-seq references. To assess the robustness of methods toward different scRNA-seq references, two alternative scRNA-seq datasets, i.e. HER2$^+$ BRCA and DCIS1 scRNA-seq datasets, were used as the reference mapped to the 10X Visium breast cancer ST sample2. **(a)** UMAP of HER2$^+$ BRCA scRNA-seq data, showing 11 cell types, including epithelial cells but not tumor cells. **(b)** UMAP of DCIS1 scRNA-seq data, showing 9 cell types including tumor cells and two types of epithelial cells. **(c)** H&E image of the 10X Visium ST sample1 with five different labeled regions. **(d)** Visualization of the mapping results by Celloc and the previous methods for all cell types and epithelial cells, using the HER2$^+$ BRCA scRNA-seq data and ST sample2 data. **(e)** Visualization of the mapping results by Celloc and the previous methods for all cell types and epithelial 1/2 subgroups, using the DCIS1 scRNA-seq data and ST sample2 data.

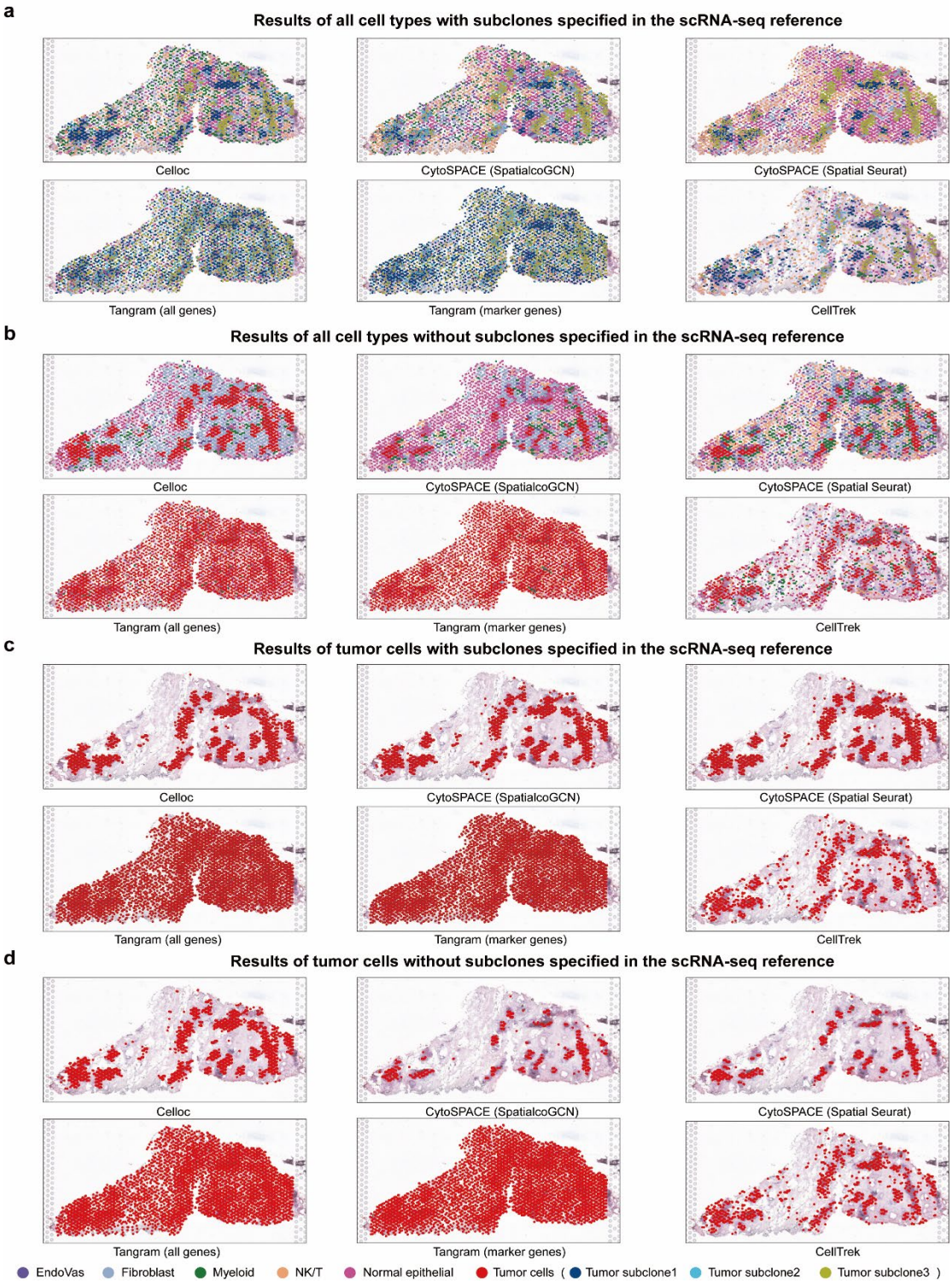

Supplementary Fig. 3. Visualization of (regular) mapping results of all cell types in DCIS dataset with and without subclone type specified in scRNA-seq reference. **(a)** Visualization of the mapping results of all cell types with subclones specified in the scRNA-seq reference. (**b**) Visualization of the mapping results of all cell types without subclones specified in the scRNA-seq reference. **(c)** Visualization of the mapping results of all tumor cells with subclones specified in the scRNA-seq reference. (**d**) Visualization of the mapping results of all tumor cells without subclones specified in

the scRNA-seq reference. Notably, CellTrek does not take cell type annotation in the scRNA-seq reference into consideration, therefore same results were obtained by Celloc using scRNA-seq references with/without the subclone type annotation.

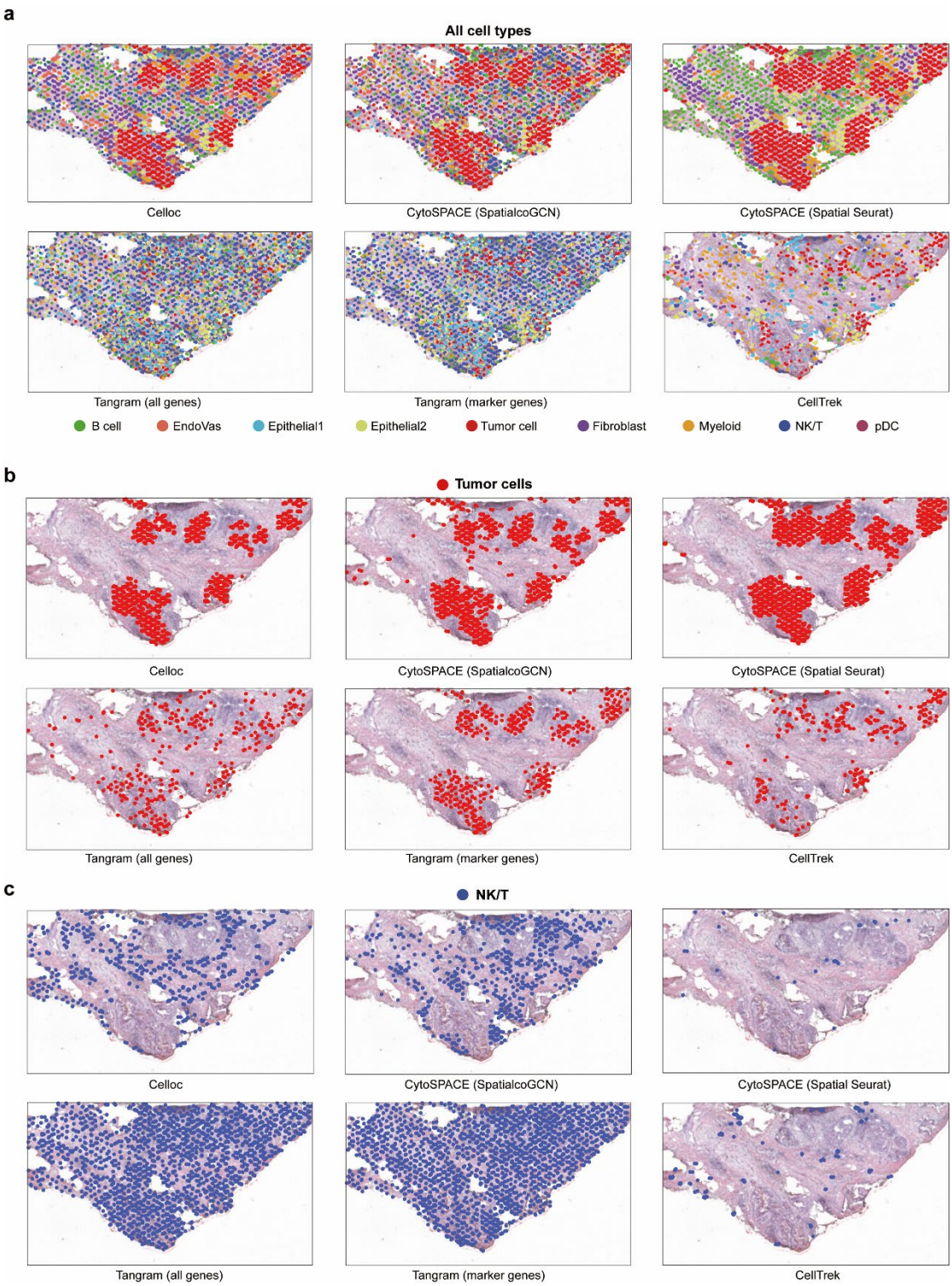

Supplementary Fig. 4. Visualization of (regular) mapping result by Celloc and the previous methods on the dataset for tumor-immune microenvironment analysis. **(a)** The mapping results of all cell types. **(b)** The mapping results of tumor cells. **(c)** The mapping results of NK/T cells.

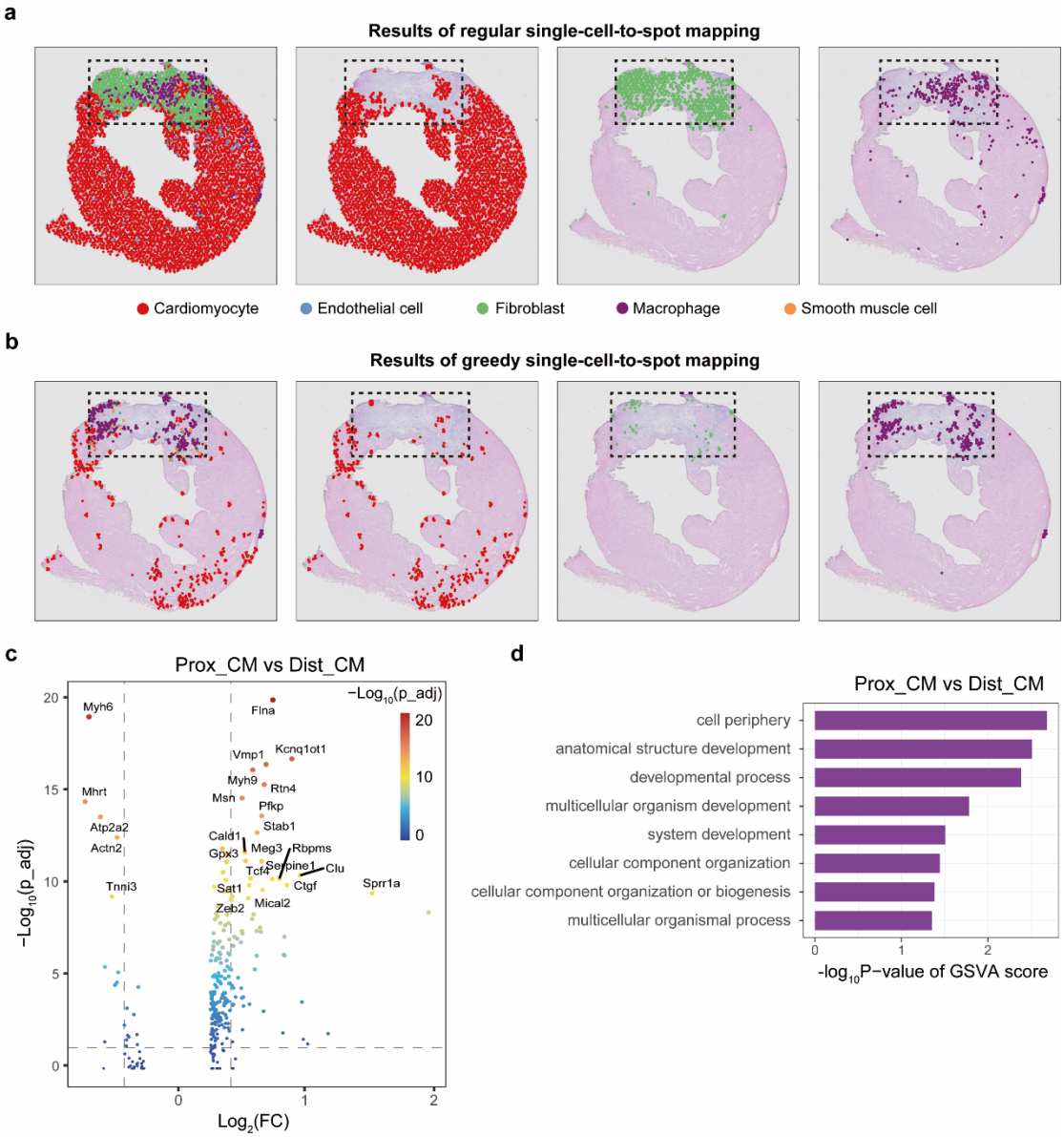

Supplementary Fig. 5. The spatial distribution and gene spatial expression patterns in myocardial infarction (MI) derived from Celloc mapping results. (a) Visualization of the spatial distribution of different cardiac cell types in the regular mapping result. The dotted box represents the infarcted area. **(b)** Visualization of the spatial distribution of different cardiac cell types in the greedy mapping result. **(c)** Differentially expressed genes between cardiomyocytes group proximal (Prox_CM) and distal (Dist_CM) to the fibrotic infarct area. More specifically, K-distance from cardiomyocytes to fibroblasts was calculated to group the cardiomyocytes based on the greedy mapping result. **(d)** Pathways showing high activities among the Prox_CM group in GSVA analysis.

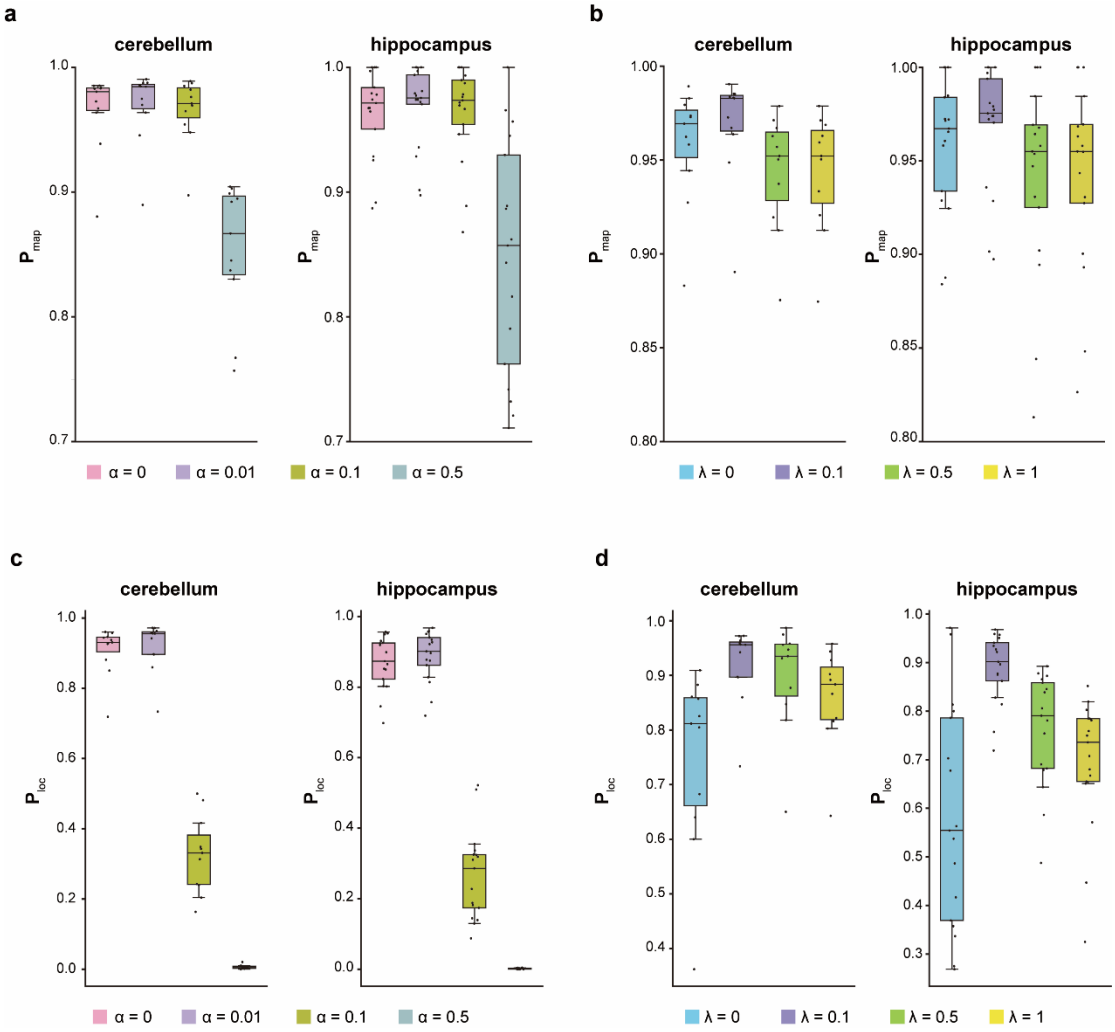

Supplementary Fig. 6. Performance of Celloc regular mapping using different term weight parameters. To control overfitting, only the simulated scRNA-seq data with 5% noise level and ST data with a mean of 5 cells per spot were used for the selection of term weight parameters. The parameters α and λ control the weight of paired distance term and cell quantity constraint term in the objective function, respectively. **(a)** The boxplots comparing mapping precision (P_{map}) in regular mapping across different α values on simulated cerebellum and hippocampus datasets. **(b)** The boxplots of mapping precision in regular mapping across different λ values on simulated cerebellum and hippocampus datasets. **(c)** The boxplots of location prediction precision (P_{loc}) in greedy mapping across different α values on simulated cerebellum and hippocampus datasets. **(d)** The boxplots of location prediction precision in greedy mapping across different λ values on simulated cerebellum and hippocampus datasets.